

Theoretical Investigation of Reaction Pathways of 3-Methyloxadiazolinium Ion and 1,2,3-Oxadiazoline: Correlation with Experimental Findings

Marilyn B. Kroeger Koepke,* Ann M. Schmiedekamp,† and Christopher J. Michejda

Molecular Aspects of Drug Design Section, ABL-Basic Research Program, NCI-Frederick Cancer Research and Development Center, Frederick, Maryland 21702

Received November 22, 1993 (Revised Manuscript Received March 31, 1994*)

Quantum mechanical calculations were used to investigate the stability of the 3-methyloxadiazolinium ion and 1,2,3-oxadiazoline and to determine the most probable thermal decomposition pathway of the oxadiazoline. *Ab initio* RHF calculations were carried out at the 3-21G and 6-31G* basis set level to obtain the optimized SCF energies and geometries of these molecules, as well as that of the protonated 4,5-dihydro-2,3-oxadiazoline. Only the N2-protonated oxadiazoline was found to be stable; the N1- and O-protonated oxadiazolines underwent immediate decomposition. Calculations on the oxadiazolinium ion confirmed experimental results regarding the most likely site of nucleophilic attack on the molecule. Sequential bond-stretching of the N-O, N-C, and O-C bonds of the optimized oxadiazoline molecule revealed that breakage of the N-O bond leading to diazomethane and formaldehyde was energetically the most favorable pathway at all levels of theory (energy of activation (E_a) of 18.8 kcal/mol at the MP2/6-31G* level). This result is consistent with the experimental finding of methylation of DNA guanine by *N*-(2-hydroxyethyl)-*N*-nitrosomethylamine [^{14}C]-labeled in the ethyl group, which has been postulated to involve the oxadiazoline as the methylating agent. Breakage of the N-C bond led to nitrogen gas and acetaldehyde as products with an E_a of 25.2 kcal/mol, while the stretching of the O-C bond led to the production of nitrous oxide and ethene with an E_a of 28.8 kcal/mol. Breakage of the N-O bond in the N2-protonated oxadiazoline occurred with an E_a of 40.0 kcal/mol, the least energetically favorable process. Optimized geometries and energies for the reactant, transition state, and product molecules were obtained at post Hartree-Fock using MP2 and QCISD, as well as the density functional code, DGauss. Comparison of the optimized geometries of the transition states from the three different bond-breakage processes revealed minor differences in these structures at the various levels of theory.

Introduction

We initiated a theoretical study of the 3-methyloxadiazolinium ion (Me-ODI) and 1,2,3-oxadiazoline (OD) in order to elucidate the properties of these molecules, as well as to ascertain the most energetically favorable pathway of decomposition of the latter compound. OD is a putative intermediate in the activation of some (β -hydroxyethyl)nitrosamines to alkylating agents.¹ OD results from methyl transfer from Me-ODI and is also produced by cyclization of (*Z*)-2-chloroethyl diazohydroxide.² These diazotates arise from the decomposition of (2-haloethyl)nitrosoureas, which are used clinically in the treatment of human malignancies, including Burkitt's lymphoma, Hodgkin's disease, and cerebral neoplasms.³⁻⁵

Considerable effort has been expended in our laboratory toward the understanding of the chemistry and biochemical aspects of metabolism of several (β -hydroxyalkyl)-nitrosamines. We have shown that one member of this class, *N*-(2-hydroxyethyl)-*N*-nitrosomethylamine (NM-

HEA), is a potent hepatocarcinogen in female F344 rats.⁶ Some years ago, we postulated that nitrosamines such as NMHEA may undergo activation to an ultimate carcinogen by conjugation of the hydroxyl group with a good leaving group such as sulfate,⁷ catalyzed by one of the sulfotransferase enzymes. NMHEA was found to alkylate rat liver DNA-guanine *in vivo* in a dose-dependent manner,⁸ giving both O⁶- and 7-methyl- and (hydroxyethyl)guanine adducts. Studies of the effect of the sulfotransferase inhibitor propylene glycol (PG) on DNA alkylation *in vivo*⁹ found that inhibition of guanine methylation by PG is consistent with the hypothesis that the methylating agent formed by activation of NMHEA is Me-ODI.

Chemical support for the sulfotransferase hypothesis was obtained when studies revealed that the *p*-toluenesulfonate (tosylate) ester of NHMEA solvolyzed very rapidly in glacial acetic acid with the formation of the corresponding acetate (Scheme 1). The large rate increase observed was explained by the participation of the *N*-nitroso group in the reaction.¹⁰ This anchimeric assistance suggested the reaction proceeded through the intermediacy of a cyclic intermediate, 3-methyloxadiazolinium tosylate. This compound could in fact be isolated

† Pennsylvania State University, Ogontz Campus, Abington, PA 19001.

* Abstract published in *Advance ACS Abstracts*, May 15, 1994.

(1) Michejda, C. J.; Koepke, S. R.; Kroeger-Koepke, M. B.; Bosan, W. In *Relevance of N-Nitroso Compounds to Human Cancer: Exposures and Mechanisms*; O'Neill, I. K., Chen, J., Bartsch, H., Eds.; Publication No. 84, International Agency for Research in Cancer: Lyon, France, 1987; pp 77-82.

(2) Brundrett, R. B. *J. Med. Chem.* 1980, 23, 1245.

(3) Proceedings of the 7th New Drug Symposium on Nitrosoureas. *Cancer Treat. Rep.* 1976, 60, 651.

(4) Singer, B.; Kusmierek, J. T. *Annu. Rev. Biochem.* 1982, 51, 655.

(5) Lown, J. W.; McLaughlin, L. W.; Chang, Y. M. *Bioorg. Chem.* 1978, 7, 47.

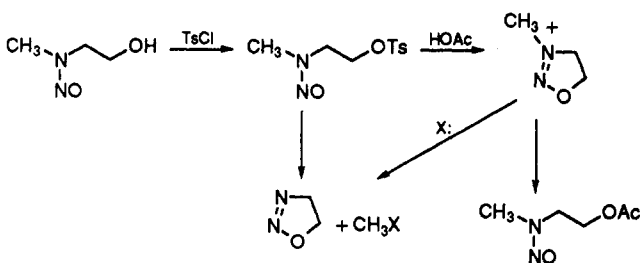
(6) Koepke, S. R.; Creasia, D. R.; Knutsen, G. L.; Michejda, C. J. *Cancer Res.* 1988, 48, 1533.

(7) Michejda, C. J.; Andrews, A. W.; Koepke, S. R. *Mutat. Res.* 1979, 67, 301.

(8) Koepke, S. R.; Kroeger-Koepke, M. B.; Bosan, W.; Thomas, B. J.; Alvord, W. G.; Michejda, C. J. *Cancer Res.* 1988, 48, 1537.

(9) Kroeger-Koepke, M. B.; Koepke, S. R.; Hernandez, L.; Michejda, C. J. *Cancer Res.* 1992, 52, 3300.

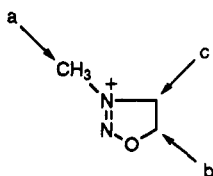
(10) Michejda, C. J.; Koepke, S. R. *J. Am. Chem. Soc.* 1978, 100, 1959.

Scheme 1. Solvolysis of the NMHEA Tosylate Ester

when a solution of NMHEA tosylate was warmed in a non-nucleophilic solvent, such as methylene chloride.¹⁰

The Me-ODI itself formed readily when NMHEA was treated with sulfur trioxide in pyridine.¹¹

It is possible for three sites on the Me-ODI to be subject to nucleophilic attack. Reaction at site b was shown to be



preferred in the acetolysis of (*S*)-*N*-nitroso-(2-hydroxypropyl)methylamine, which resulted in the formation of the corresponding (*S*)-acetate.¹² The retention of configuration in a nucleophilic displacement required a double inversion, first in the formation of the cyclic intermediate, and second in the opening of the intermediate to the final product. In a different reaction, 1 equiv of the oxadiazolium tosylate with 1 equiv of aniline in methylene chloride at room temperature produced the β -anilino derivative of NMHEA in 82% yield.¹¹ This again suggested site b is favored by this nucleophile. Loeppky et al.¹³ also found that morpholine or thiophenol in methylene chloride, but not in water, attacks site b to give a 25% yield of open chained nitrosamine. They also determined that guanine derivatives and guanine residues in DNA react with the Me-ODI to incorporate the entire nitrosamine fragment at N.⁷ These workers found no evidence of attack at site c. Studies have indicated that site a could also be attacked by an appropriate nucleophile. The reaction of the Me-ODI with 3,4-dichlorothiophenol in methylene chloride under nitrogen produced a 90% yield of 3,4-dichlorophenyl methyl sulfide.¹¹ Methylation of guanine by the oxadiazolium ion or the uncyclized tosylate was also observed when the reaction was carried out in dry dimethyl sulfoxide.¹¹ This again supports the attack of site a by the guanine nucleophile. Our studies on the reaction of NMHEA tosylate or on Me-ODI itself also failed to find any examples of nucleophilic attack at site c, nor was any evidence of a mixed reaction observed.

Theoretical studies of the Me-ODI and the OD were undertaken to help clarify some of the experimental results. The goal of these calculations was to obtain geometries and energies of the most likely reaction pathways of

decomposition of the OD at varying levels of theory and, in addition, examine the stability of the OD following protonation at various sites.

Calculations

Both semiempirical and *ab initio* methods were employed to determine the optimized geometries and equilibrium energies for the Me-ODI, 1, and OD, 2 (Scheme 2). The transition states associated with stretching the NO, the NC, and the OC bonds of 2 (structures 4, 5, and 6, respectively) and the products associated with each stretch (structures 8, 9, and 10, respectively) were calculated. In addition, the N2-protonated species of the OD, 3, and its transition state and products (7 and 11, respectively) were investigated. However, our attempts to determine a stable structure for the N1- and O-protonated species of the OD, and their respective transition states, failed.

Initial calculations on the OD molecule to obtain activation energies of bond breakage were carried out using the CAChe software (Version 3.0)¹⁴ at the PM3¹⁵ level. Further calculations utilized the Gaussian series of programs including Gaussian 90 and 92,¹⁶ adapted to run on the Cray YMP-2 computer at FCRDC. Optimized geometries of all structures were determined from Hartree-Fock calculations using the standard 3-21G and 6-31G* basis sets. Post Hartree-Fock calculations were performed using Møller-Plesset perturbation theory within the frozen core approximation at the 6-31G* basis set level (MP2/6-31G*) in order to study the effects of electron correlation on the geometries and energetics of these systems. In addition, single point energies were calculated using quadratic configuration interaction including single and double substitutions at the 6-31G* basis set level (QCISD/6-31G*) using the 6-31G* optimized geometry. Optimizations at this level could not be performed due to memory and cost efficiency limitations. Although the Berny optimization algorithm was used in the exploration of the hypersurface to find saddle points and energy minima, the analytic force field was calculated for all stationary points to verify either that they were minima or that the transition states had one negative eigenvalue. After transition states were obtained, intrinsic reaction coordinate (IRC) calculations were carried out to follow the reaction path in both directions, leading back to the reactant as well as to the products. In these calculations, the geometry is optimized at each point along the reaction path as the system decreases in energy to verify that the saddle points obtained were associated with the reaction path originally assumed. Solvent calculations were carried out with the self-consistent reaction field (SCRFF) option of Gaussian 92 using a dielectric constant of 78.2¹⁷ for water.

The potential surface calculations were also performed using density functional theory because these calculations inherently include some correlation energy contributions. These calculations were performed with the DGauss code,¹⁸ using the orbital Gaussian basis set (DZVP). In this basis set, an orbital Gaussian basis set for N, O, and C used (621/41/1) contraction patterns and (41) for H. The standard auxiliary basis set (A1) used an identical number of functions to fit both the charge density and the exchange correlation potentials. For C, N, and O these were (7/3/3; 7/3/3), respectively, and for H it was (4;4). DGauss calculations were optimized using the Vosko-Wilk-Nusair (VWN) local spin density (LSD) approximation of the exchange-correlation potential.¹⁹ DGauss transition and reactant energies were corrected by calculating the nonlocal and gradient correction

(14) CAChe software is available from CAChe Scientific, Beaverton, OR.

(15) Stewart, J. J. P. *J. Comp. Chem.* 1989, 10, 209.

(16) Gaussian 92, Revision C: Frisch, M. J.; Trucks, G. W.; Head-Gordon, M.; Gill, P. M. W.; Wong, M. W.; Foresman, J. B.; Johnson, B. G.; Schlegel, H. B.; Robb, M. A.; Replogle, E. S.; Gomperts, R.; Andres, J. L.; Raghavachari, K.; Binkley, J. S.; Gonzales, C.; Martin, R. L.; Fox, D. J.; Defrees, D. J.; Baker, J.; Stewart, J. J. P.; Pople, J. A. Gaussian, Inc., Pittsburgh, PA, 1992.

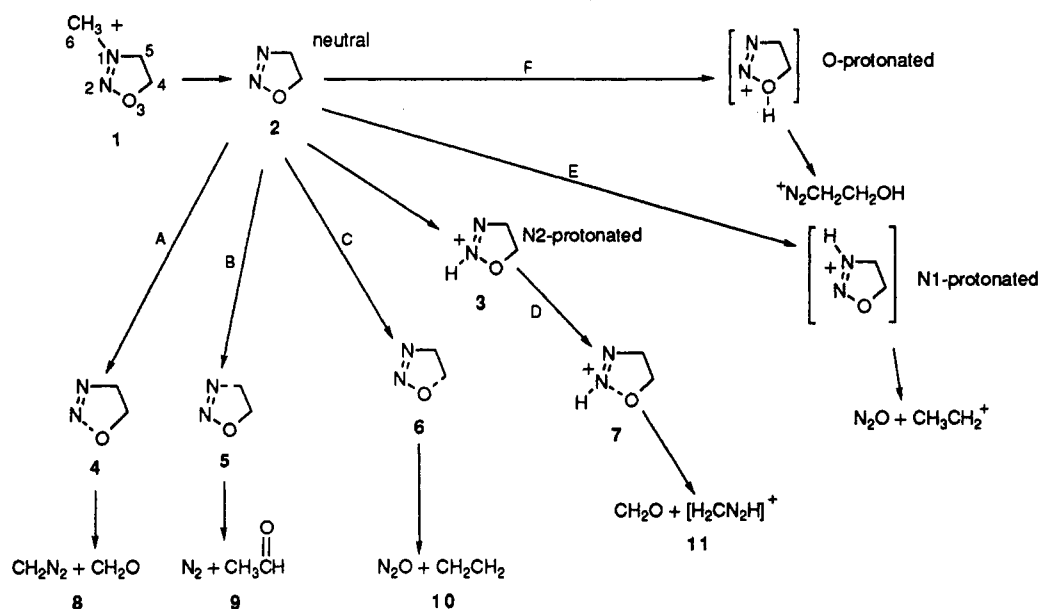
(17) The value for the dielectric constant for water at 25 °C: *Handbook of Chemistry and Physics*, 59th Ed.; Weast, R. C., Ed.; CRC Press, Inc.: West Palm Beach, FL, 1976.

(18) Andzelm, J. In *Density Functional Methods in Chemistry*; Labanowski, J. K., Andzelm, J. W., Eds.; Springer Verlag: New York, 1991; p 155. DGauss is available as part of the Unichem software package from Cray Research, Egan, MN.

(11) Michejda, C. J.; Koepke, S. R.; Kroeger-Koepke, M. B.; Hernandez, L. In *The Chemistry and Biochemistry of Nitrosamines and N-Nitroso Compounds*; Loeppky, R. N., Michejda, C. J., Eds.; ACS Symposium Series No. 553; American Chemical Society: Washington, D.C., 1994; pp 195-210.

(12) Koepke, S. R.; Kupper, R.; Michejda, C. J. *J. Org. Chem.* 1979, 44, 2718.

(13) Loeppky, R. N.; Erb, E.; Srinivasan, A.; Yu, L. In *The Chemistry and Biochemistry of Nitrosamines and N-Nitroso Compounds*; Loeppky, R. N., Michejda, C. J., Eds.; ACS Symposium Series No. 553; American Chemical Society: Washington, D.C., 1994; pp 334-336.

Scheme 2. Neutral and Protonated Structures Investigated by Computational Methods at Various Levels of ab Initio Theory**Table 1. Optimized Geometrical Parameters for 1,2,3-Oxadiazoline Neutral and Protonated Stable Molecules at the HF/6-31G*, MP2/6-31G*, and DGauss/DZVP* Levels of Theory**

structure	bond length (Å)					bond angle (deg)					
	N1-N2	O5-N2	C4-C5	O5-C4	C5-N1	C3N1N2	C4C3N1	O5C4C3	O5N2N1	C6N1N2	C3N1N2O5
1 H	1.235	1.364	1.542	1.504	1.506	115.5	100.6	102.6	111.2	120.5	0
M	1.273	1.309	1.529	1.490	1.480	114.6	100.3	103.1	111.1	119.9	0
D	1.278	1.318	1.537	1.507	1.493	114.5	100.5	102.9	111.3	120.7	0
2 H	1.210	1.469	1.542	1.463	1.508	113.7	103.1	103.4	111.7	-	0
M	1.243	1.421	1.529	1.450	1.483	111.4	103.8	103.7	113.1	-	0
D	1.241	1.442	1.524	1.462	1.494	111.9	103.7	103.6	113.2	-	0
3 H	1.207	1.419	1.554	1.505	1.513	109.2	103.8	103.5	119.1	-	0
M	1.241	1.329	1.542	1.497	1.479	105.7	105.0	102.7	122.4	-	0
D	1.242	1.360	1.555	1.499	1.479	106.5	104.9	102.9	121.7	-	0
4 H	1.094	2.241	1.825	1.265	1.423	141.9	98.1	110.1	88.5	-	0
M	1.176	2.180	2.001	1.275	1.363	142.7	94.4	108.1	91.5	-	0
D	1.147	2.346	2.156	1.249	1.333	153.6	90.9	106.3	85.6	-	-1.04
5 H	1.095	2.259	1.508	1.291	1.812	118.5	97.9	114.1	97.6	-	-4.06
M	1.166	2.154	1.472	1.300	1.861	111.2	95.6	116.6	103.2	-	-2.79
D	1.146	2.300	1.478	1.308	1.994	111.3	94.8	118.5	102.3	-	-2.95
6 H	1.141	1.226	1.378	2.036	2.023	102.3	101.8	101.1	134.6	-	0
M	1.198	1.254	1.396	1.961	1.976	100.7	103.1	101.9	133.3	-	0
D	1.176	1.219	1.371	2.249	2.117	98.6	104.1	99.8	143.5	-	0
7 H	1.160	1.997	1.936	1.260	1.364	125.8	100.9	105.9	104.2	-	0
M	1.185	2.091	2.199	1.277	1.332	137.8	93.0	104.1	100.4	-	0
D	1.190	2.179	2.173	1.242	1.314	138.3	93.5	103.5	96.6	-	3.82

^a H = Gaussian calculation at HF/6-31G* level of theory; M = Gaussian calculation at the MP2/6-31G* level of theory; D = DGauss calculation using DZVP basis set. ^b (-) = not applicable for this compound.

with the Becke (exchange)²⁰ functionals as a perturbation on the LSD optimized geometry. Since analytical second derivatives are not currently implemented in DGauss, the second derivatives were computed by finite differences of the first derivatives to verify that the transition states calculated with DGauss were maxima in the reaction coordinate.

Results and Discussion

The optimized geometrical parameters for the Me-ODI, 1, are shown in Table 1. Calculations performed at the 6-31G* basis set level revealed that either site a or b was the most susceptible for nucleophilic attack, since these atoms had the most electropositive charge (Table 2). Conversely, the calculation shows that site c is a poorer

Table 2. Atomic Charges from Mulliken Population Analysis with Hydrogens Summed into Heavy Atoms of 3-Methyloxadiazolinium Ion

atom ^a	charge ^b	atom ^a	charge ^b
C4	0.498	N1	-0.313
C5	0.363	N2	0.397
C6	0.468	O	-0.414

^a Atoms numbered according to Scheme 2. ^b Data obtained from HF/6-31G* calculations.

site for nucleophilic attack. These results verify what we have observed experimentally. Carbon 4 appears to be a softer site relative to carbon 6 (the methyl group carbon), since the nucleophiles which attack that site (aniline and acetate) are softer than those which attack the 7-position of guanine and 2,4-dinitrothiophenol.²¹

Table 3. Total Energies Calculated for the 3-Methyloxadiazolinium Ion and Neutral and Protonated 1,2,3-Oxadiazoline Reactant, Transition State, and Product Structures

structure	energy (hartrees)				
	HF/ 6-21G	HF/ 6-31G*	MP2/ 6-31G*	QCISD/ 6-31G**	DGauss/ NLSD
1	-299.4094	-301.1097	-301.9925	-302.0322	-303.0044
2	-260.2469	-261.7311	-262.4926	-262.5224	-263.3474
3	-260.5608	-262.0367	-262.7937	-262.8306	-263.6544
4	-260.1875	-261.6700	-262.4629	-262.4648	-263.3052
5	-260.1743	-261.6665	-262.4527	-262.4698	-263.3028
6	-260.1610	-261.6347	-262.4469	-262.4415	-263.2967
7	-260.4608	-261.9301	-262.7303	-262.7431	-263.5878
8	nc ^b	-261.7101 ^c	-262.4665 ^c	-262.4887 ^c	-263.3163
9	nc	-261.8600 ^c	-262.5927 ^c	-262.6243 ^c	-263.4178
10	nc	-261.7118 ^c	-262.4891 ^c	-262.4967 ^c	-263.3258
11	nc	-262.0071 ^c	-262.7509 ^c	-262.7871 ^c	-263.5697

^a Single point energy determination. ^b nc = not calculated at this basis set level. ^c Total energy summed from individual products.

Table 4. Energy of Activation and Enthalpy (kcal/mol) for 1,2,3-Oxadiazoline Bond Breakage at Different Basis Set Levels

basis set	energy of activation				enthalpy			
	A	B	C	D	A	B	C	D
PM3	34.5	48.7	56.0	nc	nc	nc	nc	nc
HF/3-21G	37.3	45.6	53.9	62.8	nc	nc	nc	nc
HF/6-31G*	27.0	29.2	49.2	70.3	18.89	-80.88	12.11	18.5
MP2/6-31G*	18.8	25.2	28.8	40.0	16.3	-62.8	21.96	26.86
QCISD/6-31G*	33.0	29.9	47.6	51.8	21.15	-63.94	16.12	27.1
DGauss/NLSD	26.5	28.0	31.8	41.8	19.5	-44.2	13.6	53.2

^a nc = not calculated at this basis set level.

Chemical studies have shown that the reaction of the Me-ODI at site a causes methylation of the nucleophile and the formation of an apparently unstable product, OD, 2. This compound is a cyclic diazotic acid ether, a molecule which would be predicted to fragment readily. In fact, calculations at both the semiempirical PM3 level and at the *ab initio* 3-21G and 6-31G* basis set levels show that the molecule is capable of existence, as has been reported previously by Sapse *et al.*²² The optimized geometrical parameters (Table 1) and SCF energies calculated at the HF/3-21G basis set level (shown in Table 3) are identical to those obtained in the earlier work.

The decomposition of OD was studied by sequential stretching of the NO, NC, or OC bonds (cases A, B, and C in Scheme 2). The results revealed that the molecule did undergo fragmentation with relative ease. In all three cases, bond-stretching ultimately led to a transition-state structure. Once the saddle point optimized geometries were obtained, IRC calculations at the 3-21G level were performed in order to follow the reaction path from the transition state in both directions (data not shown). These graphs and the calculated enthalpies (Table 4, MP2/6-31G*) revealed that while reactions A and C were endothermic, reaction B, in contrast, was highly exothermic. Geometries of the products could be optimized from the endpoint of the IRC calculations, and energies were calculated (Table III). The energies from the two products, optimized separately, were added together to obtain the values shown in Table 4. For case A, a single point

calculation of the two products separated by 5.0 Å gave an energy 0.2 kcal/mol different from the sum of the separately calculated product energies. We have therefore reported the sum of the product energies for A-C, assuming the basis set superposition error to be negligible. In the case of the DGauss calculations, the products, separated by at least 3.5 Å, could be calculated together.

The optimized 3-21G parameters were used as input for calculations at the higher 6-31G* basis set level. For all three cases, the saddle points obtained were verified by a frequency calculation, in order to ensure that only one negative eigenvalue was observed. In like fashion, the optimized geometrical parameters at the 6-31G* level were used as input for the MP2 calculations, which include a correlation energy contribution. Transition states obtained at this level were also verified by frequency calculations. The optimized geometrical parameters at all the basis set levels for the transition states are tabulated in Table 1.

Initial exploration of the activation energy of the three reaction paths for the decomposition of the oxadiazoline using the CAChe modeling software at the PM3 level showed that cleavage of the N-O bond (case A) was the most energetically favorable pathway (Table 4) (heats of formation not shown). The products from case A are diazomethane and formaldehyde (see Scheme 2). As the N-O bond length was systematically stretched, the C-C bond was also lengthened until the transition state was reached, whereupon the OD fell apart into the two products. The somewhat surprising finding that this pathway is the most favorable energetically was supported by calculations at the *ab initio* level. Total energies for all the stable optimized reactant, transition state, and product structures are shown in Table 3. These values were obtained from basic Hartree-Fock calculations, as well as from Moller-Plesset perturbation calculations and DGauss determinations. Energies of activation for all the pathways were calculated from Table 3 and are shown in Table 4. As can be seen, the higher level calculations at all levels except for the QCISD calculation verify that case A was the most energetically favorable, followed in order by cases B and C, respectively. The anomalous QCISD energy probably results from the fact that it was a single point calculation at the HF/6-31G* geometry. Unpublished results²³ from this laboratory indicate that post HF single point calculations at geometries not optimized at the same level can yield inconsistent energies. For example, we found some inconsistencies in the energy differences between two conformers of triazene (HN=NNH₂). In one conformer the saturated nitrogen is trigonal (NH₂ coplanar with the rest of the molecule), while in the other it is pyramidal. However, there were notable differences between post Hartree-Fock single point calculations (MP3 and MP4) on optimized structures obtained at a lower level. Thus, such calculation results should be viewed with some caution. It can be seen that the *E_a*'s from the MP2/6-31G* calculations were quite comparable to DGauss results, reflective of the partial inclusion of correlation energy in the latter calculation. Both of these energies of activation are lower than those of the the Hartree-Fock calculations performed at the 3-21G or 6-31G* basis set levels.

Recent interest in density functional theory, motivated by the computational efficiency of the density functional algorithm, as well as by the fact that it includes some

(19) Becke, A. D. *J. Chem. Phys.* 1986, 84, 4524.

(20) Perdew, J. P. *Phys. Rev. B* 1986, 33, 8822; erratum in *Phys. Rev. B* 1986, 33, 7406.

(21) For a review on acid/base hardness or softness see: Pearson, J. In *Advances in Free Energy Relationships*; Chapman and Shorter, Eds.; Plenum Press: New York, 1972; pp 281-319.

(22) Sapse, A.-M.; Allen, E. B.; Lown, J. W. *J. Am. Chem. Soc.* 1988, 110, 5671.

(23) Schmeidekamp, A. M. unpublished results.

contribution to the correlation energy, prompted us to apply this method to the present problem. Table 1 shows a comparison of the optimized geometry of the structures shown in Scheme 2 calculated by the three methods, HF/6-31G*, MP2/6-31G*, and DGauss/DZVP in the local spin density approximation. In the structures which represented a minimum (1-3), DGauss and MP2/6-31G* geometries are in best agreement, a trend observed by Schmiedekamp et al.²⁴ However, in the transition states (4-6), the density functional geometry from DGauss seems to "underbind" the structure, relative to Hartree-Fock and MP2. The unbonded distances (those greater than 1.8 Å) are at least 0.05-0.2 Å longer in every case than the MP2/6-31G* or HF/6-31G* distances. This may reflect the inadequacy of the local spin density approximation. DGauss transition state geometries in cases A and C (4 and 6), where the nonbonded distances are the greatest, show a molecule closer to products than the corresponding HF and MP2 structures. For instance, in case A, DGauss gives larger O3-N2 and O3-C4 distances and the C5N1N2 angle is much larger as the diazomethane separates from the formaldehyde. Case B (5) has smaller unbonded distances, and although DGauss still has the largest unbonded distances, the agreement of all bonds and angles is closer to MP2 in this transition state than in the others.

In order to further probe geometrical differences between the three OD transition state cases, we examined the molecular orbitals of the starting OD (HOMO and HOMO - 1, as well as the HOMO of the three transition states and products in cases A-C (pictures not shown). In each transition state case, there was a symmetry correlation between the HOMO - 1 of the OD with the HOMO of each transition state.

Cases A and C (Scheme 2) are readily visualized as the retroreactions of the corresponding cycloadditions. Case A leads to diazomethane and formaldehyde. Consideration of the symmetry of the LUMO of formaldehyde (an antisymmetric π^* orbital) and the HOMO of diazomethane, which is also antisymmetric with respect to the lobes on the carbon and the terminal nitrogen, indicates that the cycloaddition is allowed, and by the principle of microscopic reversibility, the retroreaction must also be allowed. The calculated difference between the LUMO (CH_2O) and the HOMO (CH_2N_2) is 0.468 hartrees (Table 5). An analogous conclusion is obtained from a correlation diagram. Orbital symmetries indicate that the HOMO of diazomethane correlates with the HOMO of the oxadiazoline, while the HOMO of formaldehyde correlates with the HOMO - 1 of the ring. The frontier molecular orbital analysis for case C gives the energy difference between the LUMO of nitrous oxide and the HOMO of ethylene to be 0.551 hartrees. The HOMO-LUMO differences between paths A and C are in qualitative agreement with the calculated enthalpy of reaction differences (Table 4). The frontier molecular orbital analysis of case B is more difficult to make since the reaction would have been symmetry forbidden were it not for the fact that as the O-N and C-N bonds are being broken there is a concomitant migration of the H-atom from the incipient carbonyl carbon to the incipient methyl group. The formation of nitrogen from OD and the synchronous migration of an H-atom to form acetaldehyde appears to be a symmetry-allowed process.

Table 5. Molecular Orbital Energies^a of Reactant, Transition State, and Product Structures of 1,2,3-Oxadiazoline

	LUMO	HOMO	HOMO-1
case A			
oxadiazoline	0.142	-0.426	-0.432
transition state	0.087	-0.351	-0.356
CH_2O	0.145	-0.436	-0.539
CH_2N_2	0.144	-0.323	-0.540
case B			
oxadiazoline	0.142	-0.426	-0.432
transition state	0.061	-0.359	-0.396
CH_3COH	0.163	-0.420	-0.507
N_2	0.172	-0.613	-0.613
case C			
oxadiazoline	0.142	-0.426	-0.432
transition state	0.095	-0.362	-0.450
CH_2CH_2	0.184	-0.374	-0.502
N_2O	0.177	-0.492	-0.492

^a Calculated at the 6-31G* level of theory; energies reported in hartrees.

The calculated enthalpies of reaction for the various processes shown in Scheme 2 can be used to calculate the heat of formation of oxadiazoline. The heats of formation of the products in reactions A-C are known.²⁵ The heat of formation of the oxadiazoline is given by the differences between the sums of the heats of formation of the products and the calculated enthalpy of reaction for the three processes. By using the enthalpies calculated at the MP2/6-31G* level (Table 4), the heats of formation of oxadiazoline were found to be 12.8, 25.8, and 10.1 kcal/mol for reactions A, B, and C, respectively. The heat of formation from reaction D could not be determined because the heat of formation of one of the products (CH_2NNH) is unknown. The correspondence between the values for reactions A and C is relatively close. The heat of formation calculated for reaction B is somewhat higher, however. That reaction is strongly exothermic at all levels of theory, and we suspect that the discrepancy between the heat of formation of oxadiazoline calculated from that reaction, as compared to reactions A and C, mirrors the uncertainty in the precise value of the calculated enthalpy. We believe that the heat of formation for the oxadiazoline calculated from reactions A and C, namely ~ 11.0 kcal/mol, is close to the correct value. It is interesting to note that the heat of formation for that species calculated from the DGauss reaction enthalpies also averages out to be 11 kcal/mol.

The frontier molecular orbital approach to the cycloaddition reactions of electron-deficient olefins with diazomethane was used previously to successfully explain the reactivity differences between various olefins.²⁶ The cycloaddition reactions of nitrous oxide with olefins (especially electron-rich ones) were studied by Bridson-Jones et al.,²⁷ and the reaction was discussed theoretically by Houk et al.²⁸ The experimental findings in ref 27 are in remarkable agreement with the present calculated data. The reaction of ethylene and nitrous oxide at 300 °C and 500 atm gave exclusively acetaldehyde and nitrogen. The oxadiazoline was postulated to be the intermediate in the reaction. Bridson-Jones et al. had a somewhat different

(25) Lias, S. G.; Bartmess, J. E.; Liebman, J. F.; Holmes, J. L.; Levin, R. D.; Mallard, W. G. *Gas-Phase Ion and Neutral Thermochemistry*. *J. Phys. Chem. Ref. Data* 1988, 17.

(26) Sustman, R.; Wenning, E.; Huisgen, R. *Tetrahedron Lett.* 1977, 877.

(27) Bridson-Jones, F. S.; Buckley, G. D.; Cross, L. H.; Driver, J. J. *Chem. Soc.* 1951, 2999.

(28) Houk, K. N.; Sims, J.; Watts, C. R.; Luskus, L. J. *J. Amer. Chem. Soc.* 1973, 95, 7301.

(24) Schmiedekamp, A. M.; Topol, I. A.; Burt, S. K.; Razafinjanahary, H.; Chermette, H.; Pfaltzgraff, T.; Michejda, C. J. *J. Comput. Chem.*, in press.

explanation for the reaction (i.e., stepwise rather than concerted), but it is clear that case B in Scheme 2 could have accounted for their observation. In a subsequent paper Bridson-Jones and Buckley²⁹ studied the reaction of trisubstituted ethylenes with nitrous oxide. The reaction of 2-methyl-2-butene gave 3-methyl-2-butanone as a main product. Smaller amounts of 2-butanone, acetone, and acetaldehyde were also formed, together with products (cyclopropanes and alkanes) which were postulated to have arisen from diazoalkanes. All these products could be rationalized from the intermediate formation of three isomeric oxadiazolines.

The protonation of the OD was examined to determine the effect of proton attachment on the decomposition of the molecule. The proton was attached to the site of interest on the previously optimized OD structure. Initial calculations at the 3-21G basis set level revealed that only the N2-protonated OD optimized to a stable structure (see Table 1 for geometrical parameters). As can be seen from this table, the geometry of the protonated molecule was not significantly different from that of the starting OD. Stretching of the N-O bond in the N2-protonated molecule (case D) again led to the attainment of an optimized transition state structure. A frequency calculation verified that only one negative eigenvalue was observed. An IRC calculation, starting from the transition state optimized parameters, was carried out to obtain product geometries from the lowest energy point. As with the OD molecule itself, the optimized geometrical parameters from the HF/3-21G calculation of the protonated OD were used as input for calculations at the higher HF/6-31G* level of theory. The optimized structural parameters obtained from this calculation were then utilized for the MP2 calculation. The calculated energy of activation for this pathway (Table 4) was the least favorable energetically at all levels of theory. The proton affinity for protonation can be calculated by subtracting the total energy of the neutral molecule from the total energy of the cation. For the N2-protonated case, the numbers were determined to be 197.0 kcal/mol at the 3-21G basis set level and 206.5 kcal/mol at the 6-31G* level. These values are comparable to those obtained for protonation of the N2 of 4,5-dihydro-1,2,3-triazole.³⁰

Protonation of either the other ring nitrogen N1 (path E) or the oxygen (path F) did not result in stable structures (see Scheme 2). It should be noted that path E gives rise to the ethyldiazonium ion, which should ethylate DNA in experiments involving Me-ODI. However, this product was not observed on our experiments⁹. It should be stressed, however, that we know nothing about the reaction path to the final products since the N-1 protonated structure is not stable. When the oxygen atom of the OD was protonated, the molecule immediately fell apart to the (hydroxyethyl)diazonium ion. This result is consistent with the protonation behavior of the isoelectronic molecule, 4,5-dihydro-1,2,3-triazole.³⁰ The proton-induced decomposition of OD, especially by path F, may be an important route of decomposition when the concentration of H₃O⁺ is sufficiently high.

It must be kept in mind that all these calculations have been carried out in the gas phase and the molecules may have different stabilities in the presence of solvent. It was possible that the O- and N1-protonated OD molecules

could be stable in a water environment. To test this, a preliminary solvent calculation of the N1- and O-protonated ODs revealed that these molecules were indeed stable in the presence of water (HF/6-31G* energy = -262.0662 hartrees for the N1- and -262.1156 for the O-protonated OD). The calculations also revealed that for the N2-protonated OD, the presence of water did not change the energy significantly. However, the OD itself was found to be more stable by 14.1 kcal/mol in the water environment (HF/6-31G* = -261.7355 hartrees for the SCRF calculation compared with -261.7131 for the gas-phase calculation). It is therefore apparent that calculations performed in the absence of solvent may give somewhat different results than in a system which is surrounded by a dielectric.

The fact that case A is the most energetically favorable is supported by experimental biochemical data.¹¹ Treatment of calf thymus DNA with [¹⁴C-ethyl]NMHEA in the presence of a rat liver cytosol activating system and the sulfotransferase cofactor 3'-phosphoadenosine 5'-phosphosulfate (PAPS) caused *methylation* of guanine. This product was not found in the absence of PAPS. While guanine methylation was the expected result when the NMHEA was labeled in the methyl group, the detection of methylation from the [¹⁴C-ethyl]-labeled NMHEA was unexpected. Diazomethane is known to be a methylating agent for DNA guanine.³¹ Our theoretical calculations provide an explanation for this experimental result, since it suggests that diazomethane can arise as a decomposition product of the OD. Preliminary data on the alkylation of calf thymus DNA with the clinically important drug bis-(2-chloroethyl)nitrosourea (BCNU) at pH 7.0 did not show any methylation of DNA-guanine. However, a similar experiment carried out at pH 8.5 revealed extensive methylation of guanine (L. Taneyhill, unpublished data). We suspect that at pH 7.0 the hydronium ion-catalyzed decomposition of OD (pathway F, Scheme 2) is the predominant mode of decomposition, but at the higher pH, fragmentation to diazomethane and formaldehyde (case A) becomes a competitive reaction.

In conclusion, the computational results indicate the mechanism of decomposition of the elusive OD. The principal pathway leads to diazomethane and formaldehyde. These data are supported by some experimental findings. It should be possible to detect diazomethane from any reaction which involves the formation of (*Z*)-2-chloroethyl diazohydroxide.

Acknowledgment. The authors wish to thank Dr. David Bolton of CAChe Scientific for conducting the initial calculations on OD, as well as Dr. Jack Collins of the Structural Biochemistry Program in the Frederick Biomedical Supercomputing Center at NCI-FCRF for helpful discussions. Research was sponsored by the National Cancer Institute, DHHS, under Contract No. NO1-CO-74101 with ABL. We acknowledge the National Cancer Institute for the allocation of computer time and staff support at the Frederick Biomedical Supercomputer Center of the Frederick Cancer Research and Development Center. The contents of this publication do not necessarily reflect the views or policies of the Department of Health and Human Services, nor does mention of trade names, commercial products, or organizations imply endorsement by the U. S. Government.

(29) Bridson-Jones, F. S.; Buckley, G. D. *J. Chem. Soc.* 1951, 3009.

(30) Wladkowski, B. D.; Smith, R. H., Jr.; Michejda, C. J. *J. Amer. Chem. Soc.* 1991, 113, 7893.

(31) Smith, R. H., Jr.; Koepke, S. R.; Tondeur, Y.; Denlinger, C. L.; Michejda, C. J. *J. Chem. Soc., Chem. Commun.* 1985, 936.